

Chapter 2: Modulation of Sarcoplasmic Reticulum Function by PST2744 [Istaroxime; (E,Z)-3-((2-Aminoethoxy)imino) Androstane-6,17-dione Hydrochloride] in a Pressure-Overload Heart Failure Model

M Rocchetti, M Alemanni, G Mostacciolo, P Barassi, C Altomare, R Chisci, R Micheletti, P Ferrari, A Zaza

The Journal of Pharmacology and Experimental Therapeutics
Year 2008; Volume 326; Pages 957-965

Abstract

Objective: Istaroxime (PST2744) is a novel inotropic agent which enhances SERCA2 activity. We investigated istaroxime effect on Ca^{2+} handling abnormalities in myocardial hypertrophy/failure (HF^{*}).

* Abbreviations used in the chapter: ANOVA - analysis of variance; AoB - aortic banding; a.u. - arbitrary unit(s); Ca_f - free cytosolic Ca^{2+} concentration; Ca_{rest} - resting Ca^{2+} at -80 mV; Ca_{SRT} - total sarcoplasmic reticulum Ca^{2+} content; CICR - Ca^{2+} -induced Ca^{2+} release; C_m - membrane electrical capacity; CV - coefficient(s) of variation; $d\text{Ca}/dt_{\text{max}}$ - maximum velocity of Ca^{2+} rise; HF - heart failure; HW/BW - heart to body weight ratio; $I_{\text{Ca,L}}$ - L-type Ca^{2+} current; I_m - membrane current; I_{NCX} - $\text{Na}^+/\text{Ca}^{2+}$ exchanger current; L_{cyt} - liters of cytosol; LW/BW - lung to body weight ratio; NCX - $\text{Na}^+/\text{Ca}^{2+}$ exchanger; PLB - phospholamban; PST2744 - (E,Z)-3-((2-aminoethoxy)imino) androstane-6,17-dione hydrochloride; RyR - ryanodine receptor; SERCA - sarco(endo)plasmic Ca^{2+} ATPase; SR - sarcoplasmic reticulum; τ_{decay} - time constant of Ca^{2+} transient relaxation

Methods: guinea-pig myocytes were studied 12 weeks after aortic banding (AoB) and compared to those of sham-operated animals (sham). The gain of calcium-induced Ca^{2+} release (CICR), sarcoplasmic reticulum (SR) Ca^{2+} content, $\text{Na}^+/\text{Ca}^{2+}$ exchanger (NCX) function and the rate of SR reloading after caffeine-induced depletion (SR Ca^{2+} uptake, measured during NCX blockade) were evaluated by measurement of cytosolic Ca^{2+} and membrane currents. **Results:** HF characterization: AoB caused hypertrophy and failure in 100% and 25% of animals respectively. While CICR-gain during constant pacing was preserved, SR Ca^{2+} content and SR Ca^{2+} uptake were strongly depressed. Resting Ca^{2+} and the slope of the $I_{\text{NCX}}/\text{Ca}^{2+}$ relationship were unchanged by AoB. Istaroxime effects: CICR gain, SR Ca^{2+} content and SR Ca^{2+} uptake rate were increased by istaroxime in sham myocytes and, to a significantly larger extent, in AoB myocytes; this led to almost complete recovery of SR Ca^{2+} uptake in AoB myocytes. Istaroxime increased resting Ca^{2+} and the slope of the $I_{\text{NCX}}/\text{Ca}^{2+}$ relationship similarly in sham and AoB myocytes. Istaroxime failed to increase SERCA activity in skeletal muscle microsomes devoid of phospholamban. **Conclusions:** Clear-cut abnormalities in Ca^{2+} handling occurred in this model of hypertrophy with mild decompensation. Istaroxime enhanced SR function more in HF myocytes than in normal ones; almost complete drug-induced recovery suggests a purely functional nature of SR dysfunction in this HF model.

Introduction

Positive inotropic interventions remain essential in the management of heart failure; nonetheless their use is strongly limited by proarrhythmic effects and increased oxygen consumption. We have shown that, in normal myocytes, the positive inotropic effect of Na^+/K^+ pump inhibition can be dissociated from proarrhythmia if SERCA2 is stimulated¹. The two actions are simultaneously exerted by the compound (E,Z)-3-((2-Aminoethoxy)imino) androstane-6,17-dione hydrochloride (istaroxime, formerly PST2744) whose therapeutic index (inotropy/proarrhythmia) largely exceeds the one of digoxin in single cell and whole animal studies^{2;3}. The favorable therapeutic profile of istaroxime has been confirmed in animal models of heart failure^{4;5} and in man⁶. However, whether this can still be attributed to SERCA2 stimulation is an open question.

Dysfunction of the sarcoplasmic reticulum (SR) is a key feature in myocardial remodelling and is considered as a central mechanism in a wide spectrum of hypertrophy/failure etiologies. Such functional impairment has been variably attributed to downregulation of SERCA2 protein transcription and/or to an increase in the inhibitory (unphosphorylated) form of phospholamban (PLB)⁷. Thus, the expression and conformation of the molecular target of istaroxime may be changed in the failing myocardium, with unknown consequences on its effect. At a more general level, the question is how molecular remodelling may affect the response of drugs acting through SERCA2 modulation.

The present study aims to test whether istaroxime is capable of stimulating SR Ca^{2+} uptake also in the presence of cardiac

hypertrophy/failure. To this end modulation of Ca^{2+} handling by istaroxime was tested in an experimental model of cardiac dysfunction in which chronic pressure overload was induced by aortic constriction in the guinea-pig. The results obtained show that SR impairment can be largely reversed by pharmacological means in this model. This leads to a “functional” interpretation of SERCA2 abnormality, potentially relevant to the therapy of contractile dysfunction. Such an interpretation suggests that istaroxime may act by preventing the interaction between SERCA and PLB. To obtain a preliminary evaluation of this hypothesis, we also tested istaroxime effect on SERCA activity in skeletal muscle microsomes devoid of PLB. This collateral observation is reported in the Supplemental Material.

Methods

The investigation conforms to the Guide of the Care and Use of Laboratory Animals published by the US National Institutes of Health (NIH publication No. 85-23, revised 1996) and to the guidelines for animal care endorsed by the hosting institution.

Aortic banding model

Chronic pressure overload was induced in guinea-pigs after banding of the ascending aorta (AoB) under ketamine (100 mg/Kg)-xylazine (5 mg/Kg) intraperitoneally. Sham operated littermates (sham) were used as controls.

Myocyte preparation and recording solutions

Guinea-pigs were killed by cervical dislocation under ketamine-xylazine anesthesia 12 weeks (w) after AoB. Cardiac

hypertrophy/heart failure was evaluated through the heart weight/body weight (HW/BW) and lung weight/body weight (LW/BW) ratios. Ventricular myocytes were isolated by using a retrograde coronary perfusion method previously published⁸, with minor modifications. Rod shaped, Ca²⁺ tolerant myocytes, were used within 12 h from dissociation.

During measurements myocytes were superfused at 2 ml/min with Tyrode solution containing (mM) 154 NaCl, 4 KCl, 2 CaCl₂, 1 MgCl₂, 5 HEPES-NaOH, 5.5 D-glucose, adjusted to pH 7.35. The pipette solution contained (mM) 110 K⁺-aspartate, 23 KCl, 0.2 CaCl₂ (calculated free-Ca²⁺ = 10⁻⁷ M), 3 MgCl₂, 5 HEPES KOH, 0.5 EGTA KOH, 0.4 GTP-Na salt, 5 ATP-Na salt, 5 creatine phosphate Na salt, pH 7.3. Tyrode and pipette solutions were modified for the SR reloading protocol, as detailed in the section on experimental protocols (below). A thermostated manifold, allowing for fast (electronically timed) solution switch, was used for cell superfusion. All measurements were performed at 35 ± 0.5 °C.

Throughout the present study, istaroxime was tested at the concentration of 4 µM, corresponding to the steep portion of the concentration-response curve for inotropy² and shown to be effective on SR function of normal myocytes of the same species¹.

Electrophysiology techniques

Ventricular myocytes were voltage-clamped in the whole-cell configuration (Axopatch 200-A, Axon Instruments). Membrane capacitance (C_m) and series resistance were measured in every cell, but left uncompensated; the average values of series resistance in

sham and AoB experiments were $5.1 \pm 0.2 \text{ M}\Omega$ ($N = 48$) and $5.0 \pm 0.2 \text{ M}\Omega$ ($N = 63$) (N.S.) respectively. Current signals were filtered at 2 kHz and digitized at 5 kHz (Axon Digidata 1200). Trace acquisition and analysis was controlled by dedicated software (Axon pClamp 8.0). Guinea-pig ventricular myocytes do not express I_{to} (ref. ⁹); thus, peak inward current measured upon depolarizations from a holding potential of -40 mV (I_{Na} fully inactivated) essentially reflects Ca^{2+} influx (through I_{CaL} and I_{NCX}); this was confirmed in preliminary experiments (see Supplemental Figure 1). It is fair to stress that inward current, albeit adequate to calculate CICR-gain (see below), cannot be assumed to reflect I_{CaL} . Indeed, accurate measurement of I_{CaL} requires series resistance compensation, estimation of time-dependent run-down, and intracellular K^+ substitution by Cs^+ , none of which was implemented in the present experiments. In particular, K^+ substitution by Cs^+ was avoided because it affects SR function¹⁰, the main object of this study.

Measurements of intracellular Ca^{2+}

Single myocyte intracellular Ca^{2+} activity was measured fluorimetrically using the membrane permeable dye Indo1-AM (8 μM , Molecular Probes, The Netherlands) as previously described. Indo1-AM fluorescent emission was measured at two wavelengths (410 and 490 nm)¹¹. The signals at the two wavelengths (F_{410} and F_{490}) were separately lowpass filtered (200 Hz) and digitized at 2 kHz. Cytosolic Ca^{2+} activity was calculated from the F_{410}/F_{490} ratio after lowpass digital filtering (FFT, 100 Hz) and subtraction of the background luminescence. Conversion of F_{410}/F_{490} ratio to free cytosolic Ca^{2+}

concentration (Ca_f) was performed as described by Sipido et al¹² after dye calibration in ionomycin permeabilized myocytes¹.

Measurement of SERCA activity in SR microsomes

The methods for this set of experiments are reported in the Supplemental Material, where the relevant results are also presented.

Experimental protocols

Protocol 1 (Caffeine pulse protocol): Transmembrane current (holding potential -80 mV) and cytosolic Ca^{2+} were simultaneously recorded (in Tyrode solution) during a 5 s caffeine pulse (10 mM) applied 10 s after a loading train of voltage-steps (-40 to 0 mV, 200 ms, 0.37 Hz).

Protocol 2 (SR reloading protocol): the Na^+/Ca^{2+} -exchanger (NCX) was inhibited by 30 min cells incubation in a Na^+ and Ca^{2+} free solution (replaced by equimolar Li^+ and 1 mM EGTA). SR was initially depleted by a brief caffeine pulse (with 154 mM Na^+ to allow Ca^{2+} extrusion through the NCX) and then progressively reloaded by a train of depolarizing pulses (-40 to 0 mV, 200 ms, 0.25 Hz) in the presence of 1 mM Ca^{2+} (protocol outline at the top of fig 2). The pipette solution was Na^+ -free (Na^+ salts were replaced by K^+ - or Tris-salts).

Estimation of functional parameters

Total SR Ca^{2+} content (Ca_{SRT} in μ moles per liter of cytosolic volume) was estimated by integrating the Na^+/Ca^{2+} exchanger current (I_{NCX}) elicited by the caffeine pulse (protocol 1) and dividing the nmoles of Ca^{2+} by the estimated cell volume ($C_m/6.44$)¹³ (table 1).

I_{NCX} was defined as the transient component of caffeine-induced membrane current; thus, the steady state current present during caffeine superfusion (pedestal) was subtracted before integration.

The NCX function was evaluated by plotting I_{NCX} as a function of Ca_f during caffeine pulses (protocol 1, for details see fig 4). The slope of this relation was obtained by linear interpolation of the points in the final third of Ca^{2+} transient relaxation, when bulk cytosolic Ca_f values more closely reflect subsarcolemmal ones¹³ (cells in which the $I_{\text{NCX}}/\text{Ca}_f$ relation was entirely non-linear were not used for this analysis). The steady-state value of Ca_f measured at holding potential just before caffeine application will be referred to as “resting” Ca^{2+} (Ca_{rest}).

The Ca^{2+} -uptake function of SR (SERCA2 uptake flux minus leak flux) was dynamically tested by the SR reloading protocol (protocol 2). The rate of SR reloading was determined from the increment of Ca^{2+} transient amplitude in subsequent voltage steps delivered after caffeine-induced depletion. The time constant of Ca^{2+} transient relaxation (τ_{decay}), reflecting the rate of net SR Ca^{2+} uptake, was measured during each step of the reloading process by monoexponential fit of the Ca^{2+} transient decay. In consideration of the dependency of SERCA2 activity from cytosolic Ca^{2+} (ref. ¹⁴), τ_{decay} was also plotted as a function of peak Ca_f achieved during each step (see Supplemental Figure 2).

The amplification factor in Ca-induced-Ca release (CICR-gain) was calculated according to two methods. In the first one, peak amplitude of Ca^{2+} transient was divided by “peak inward current”; in the second one the maximum velocity of Ca^{2+} rise ($d\text{Ca}/dt_{\text{max}}$) was divided by

“peak inward current”. Both methods use “peak inward current” in lieu of Ca^{2+} influx, thus yielding a value in arbitrary units¹³. This approach was preferred because an absolute estimate of CICR-gain was beyond the aims of this study and the peak value of inward current may more accurately reflect Ca^{2+} influx under the present experimental conditions. It should be stressed that, because Ca^{2+} release and Ca^{2+} influx are linearly related¹³, their ratio is independent of their absolute value.

Substances

Stock Indo1-AM solution (1 mM in dry DMSO) was diluted in Tyrode solution. Istaroxime was dissolved in water. Istaroxime (PST2744, chemical structure in ref. ^{2,3} was synthesized at Prassis Sigma-Tau (Settimo Milanese, Italy), Indo-1AM from Molecular Probes (Leiden, The Netherlands), all other chemicals from Sigma (St. Louis, MO, U.S.A.).

Statistical analysis

Sham and AoB conditions are represented by distinct experimental groups; to minimize the effect of inter-subject variability, data were collected from >5 animals in each condition. Sham and AoB animals were studied in alternate sequence. Individual means were compared by paired or unpaired t- test as appropriate; in the SR loading protocol (Figs 2, 6 and Supplemental Figure 2) differences were tested by two-way ANOVA, applied to either absolute values or istaroxime-induced changes. Statistical significance was defined as $p < 0.05$ (N.S. = not significant). The least-square method was used for linear and non-

TABLE 1
Glossary of symbols and method of calculation

Symbol	Meaning	Formula	Parameters	References
Ca_f	Free cyt. Ca^{2+} (molar concentration)	$K_d \times \beta \times \frac{R - R_{\min}}{R_{\max} \times R}$	$K_d = 250 \text{ nM}; R_{\min} = 0.24;$ $R_{\max} = 0.86; \beta = 2.54$	11 from dye calibration
Ca_{NCX}	Ca^{2+} through I_{NCX} (moles)	$1/zF \times \int dI_m \times dt$	$z = 1; F = \text{Faraday constant}$	13
Ca_{SR}	SR Ca^{2+} content (moles/Lcyt.)	$\frac{Ca_{\text{NCX}}}{V_{\text{cyt}}}$	Ca_{NCX} from caffeine pulse; $V_{\text{cyt}} = C_m/6.44$	13

cyt., cytosol; I_m , membrane current; K_d , dissociation constants; R_{\min} , R_{\max} , and β , indo-1 calibration parameters 11; V_{cyt} , volume of cytosol.

TABLE 2
AoB model parameters

	HW/BW	CV	LW/BW	CV	C_m	CV
	<i>g/kg</i>		<i>g/kg</i>		<i>pF</i>	
Sham ($N = 8$)	4.37 ± 0.24	0.16	5.24 ± 0.32	0.17	216 ± 14 ($n = 48$)	0.46
AoB ($N = 12$)	$6.56 \pm 0.50^*$	0.25	5.95 ± 0.82	0.50	303 ± 14 ($n = 63$)*	0.38

* $P < 0.05$ vs. sham animals; $N = \text{no. of animals}; n = \text{no. of cells}.$

linear fitting and parameter estimation. Data are expressed as mean \pm standard error of independent determinations; the coefficient of variation (CV) was calculated as the ratio between standard deviation and mean. Sample size (number of cells) is specified for each experimental condition in the tables and figure legends.

Results

The evaluations included in this study required the development and characterization of a model of aortic banding in the guinea pig, whose effects have not been previously described. In this section, the observations concerning the functional characterization of the model will be reported first and will be followed by the description of istaroxime effects in sham and AoB animal groups. Results concerning the effect of istaroxime on SERCA activity in microsomes are reported in the Supplemental Material.

Functional characterization of the AoB model

This section of results compares myocardial function of animals 12w after AoB to that of sham of the same gender.

The heart/body weight ratio (HW/BW), lung/body weight ratio (LW/BW) and C_m of sham and AoB animals are compared in table 2. The HW/BW ratio was significantly increased by AoB. There was a tendency to increase of the LW/BW ratio in AoB; while, due to the large scatter, this change did not achieve statistical significance, in 25% of AoB animals the LW/BW ratio was more than 2 fold the

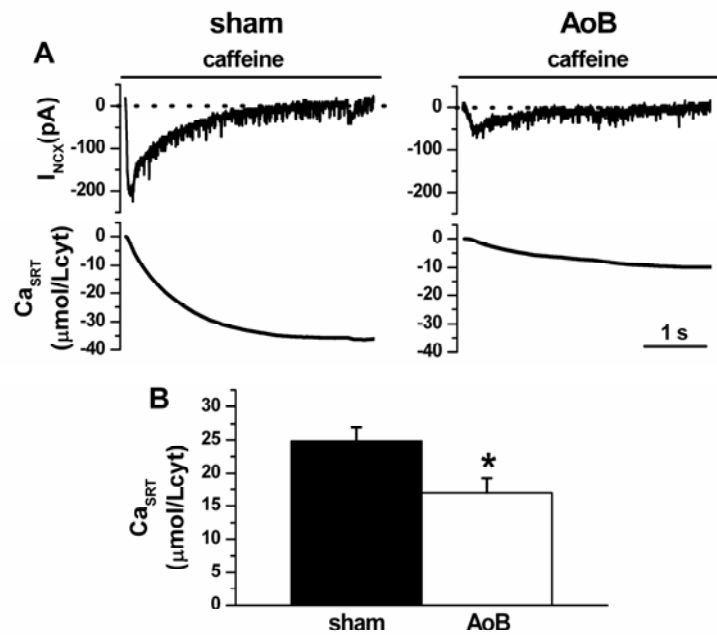


Figure 1: AoB effect on total SR Ca²⁺ content (Ca_{SRT}). A) Representative examples of caffeine-induced Na⁺/Ca²⁺ exchanger current (I_{NCX}) (holding potential -80 mV) and the corresponding cumulative I_{NCX} integrals in a sham (left panels) and AoB (right panels) myocyte. B) Average results of Ca_{SRT}, (see table 1 for method), in sham (N = 30) and AoB (N = 28) myocytes; * = p<0.05 vs sham.

average of sham animals. C_m was significantly larger after AoB, to indicate an increase in cell size. Within the study period, mortality was null in both sham and AoB groups.

As shown in figure 1, Ca_{SRT} was decreased by approx 32% after AoB ($p < 0.05$ vs sham) (Fig 1B).

During the SR reloading protocol, the parameters of Ca^{2+} transients (amplitude and τ_{decay}) and the CICR-gain changed over subsequent depolarizing pulses (Fig 2), reflecting a progressive increase in the SR Ca^{2+} content. Thus, the analysis of the time course of these parameters provides information on the SR Ca^{2+} uptake function¹. After AoB the time courses of Ca^{2+} -transient amplitude and CICR-gain were markedly slowed as compared to sham animals; τ_{decay} was uniformly increased over the whole reloading train (Fig 2B). Differences between sham and AoB myocytes in the time-course of all variables were significant ($p < 0.05$), as tested by two-way ANOVA. The change in τ_{decay} was evident also when compared at similar cytosolic Ca^{2+} concentrations (measured at the beginning of the decay of Ca^{2+} transient, see the Supplemental Figure 2). The changes in Ca^{2+} transient amplitude occurring during the loading protocol and between sham and AoB myocytes (Fig 2A) are accompanied by changes in amplitude and inactivation rate of inward current, as expected from Ca^{2+} -dependent inactivation of I_{CaL} (ref. ¹⁵).

In contrast to the marked depression of SR function detected by the reloading protocol (protocol 2), during steady state stimulation in normal Tyrode (protocol 1) the amplitudes of V-induced Ca^{2+}

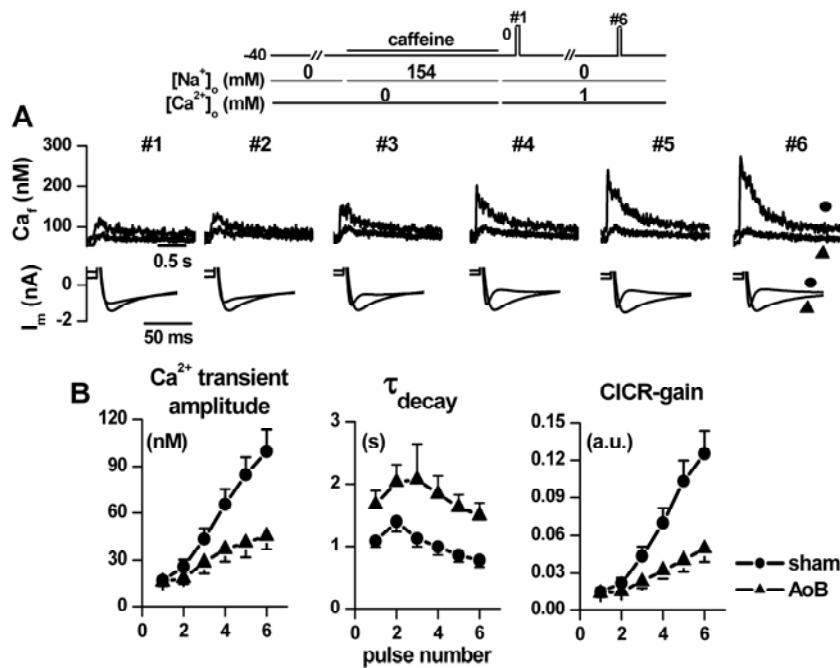


Figure 2: AoB effect on SR function (with blocked NCX). A) Example of free cytosolic Ca^{2+} concentration (Ca_i) and membrane current (I_m) recorded during SR reloading after caffeine-induced SR depletion in sham (●) and AoB (▲) myocytes; recordings were performed in the absence of NCX function (Na^+ free Tyrode and pipette solutions). B) Average values of Ca^{2+} transient parameters measured during each pulse (#1 to #6) of the stimulation train in sham (●, N = 23) and AoB (▲, N = 22) myocytes. CICR-gain (measured as the ratio between the Ca^{2+} transient amplitude and the peak inward current) was expressed in arbitrary units (a.u.) (see Methods). Inset: outline of the experimental protocol. Significance of AoB-induced changes was detected by two-way ANOVA ($p < 0.05$ for all variables).

transients (111.2 ± 11 nM vs. 106.8 ± 9 nM, N.S.), their dCa/dt_{max} (12.7 ± 1.3 nM/ms vs. 13.0 ± 1.0 nM/ms, N.S.) and peak inward current (-4.44 ± 0.32 nA vs. -3.99 ± 0.36 nA, N.S.) were similar between sham and AoB myocytes. Accordingly CICR-gain was unchanged between the two conditions, independently of the method used for its evaluation (Fig 3). The slope of the I_{NCX}/Ca_f relation and Ca_{rest} were unchanged by AoB (Fig 4).

Istaroxime effects in sham vs AoB groups

Istaroxime ($4 \mu\text{M}$) was acutely applied to myocytes from sham and AoB groups and evaluation of functional parameters was performed as above.

In sham myocytes istaroxime effects were similar to those previously reported for normal guinea-pig myocytes^{1,16}. Istaroxime increased SR Ca^{2+} content by $79.2 \pm 21.1\%$ ($p < 0.05$ vs control; Fig 5). Stimulation of SR Ca^{2+} uptake function by istaroxime was also evident during the SR reloading protocol, in which NCX contribution was absent (see methods, protocol 2). Indeed, the rate of change of Ca^{2+} transient amplitude and CICR-gain during the reloading process was increased and τ_{decay} was shortened by the drug (Fig 6). Differences between baseline and istaroxime superfusion in the time-course of all variables were significant ($p < 0.05$), as tested by two-way ANOVA. Consistently with stimulation of SR uptake function, istaroxime increased CICR-gain measured under normal Tyrode superfusion (functioning NCX, Fig 7); istaroxime also increased the

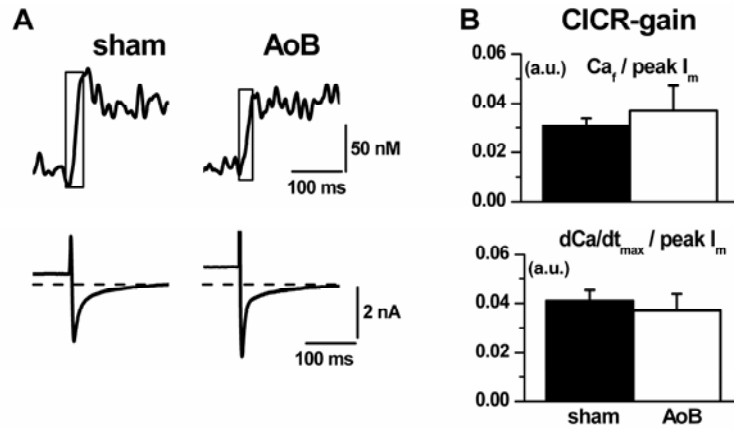


Figure 3: AoB effect on CICR-gain. A) Free cytosolic Ca²⁺ concentration (Ca_i) and membrane current (I_m) simultaneously recorded during voltage steps (from -40 to 0 mV for 200 ms) in a sham (left panels) and AoB (right panels) myocyte. B) Average values of CICR-gain (calculated according to two methods and expressed in arbitrary units, a.u., see Methods) in sham (N = 33) and AoB (N = 27) myocytes; dCa/dt_{max} was calculated during the rising phase of the Ca²⁺ transient (boxes in panel A).

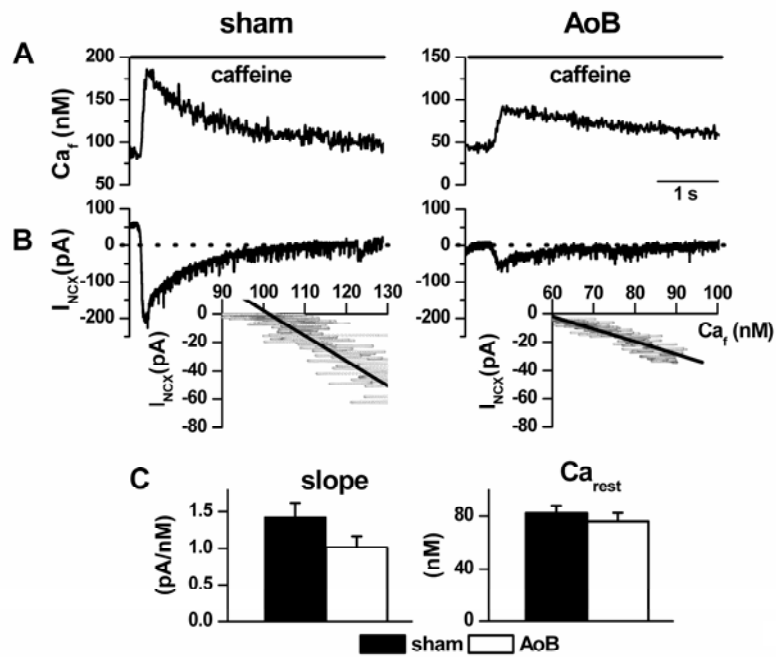


Figure 4: AoB effect on NCX function. A), B) Free cytosolic Ca²⁺ concentration (Ca_f) and the Na⁺/Ca²⁺ exchanger current (I_{NCX}) simultaneously recorded during caffeine superfusion (holding potential -80 mV) in a sham (left panels) and AoB (right panels) myocyte; I_{NCX}/Ca_f relationship and the linear interpolation of the points in the final third of Ca²⁺ transient relaxation (continuous line) are shown in the insets. C) Average results of the slope of the I_{NCX}/Ca_f relationship and resting Ca²⁺ measured at -80 mV (Ca_{rest}) in sham (N = 24) and AoB (N = 24) myocytes.

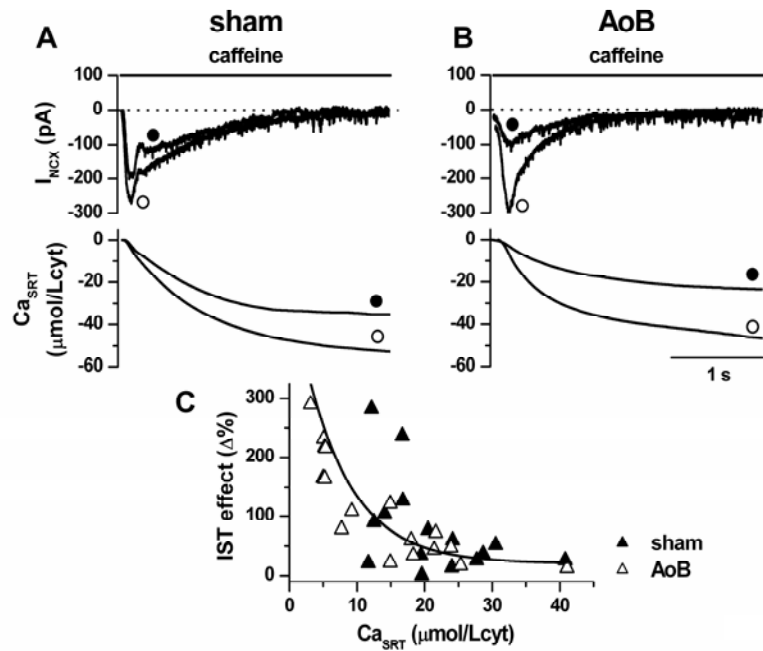


Figure 5: Istaroxime effects in sham vs AoB groups: total SR Ca²⁺ content (Ca_{SRT}). A), B) Representative example of istaroxime (IST 4 μM, ○) effect on caffeine-induced Na⁺/Ca²⁺ exchanger current (I_{NCX}) (holding potential -80 mV) and the corresponding cumulative I_{NCX} integrals in a sham and AoB myocyte. C) IST effect (Δ% increase of Ca_{SRT}) as a function of Ca_{SRT} level measured in control (cont, ●) in all experimental conditions (data from sham (▲, N = 15) and AoB (△, N = 18) groups were pooled together); continuous line represents the best exponential fit of the experimental data.

slope of the I_{NCX}/Ca_f relationship by $93.3 \pm 35 \%$ ($p < 0.05$ vs. control, Fig 8) and Ca_{rest} by $41.3 \pm 9.9\%$ ($p < 0.05$ vs. control, Fig 8).

After AoB istaroxime increased Ca_{SRT} by an average of $136.9 \pm 31.9 \%$ ($p < 0.05$); although apparently larger, this effect was not significantly different from that observed in sham myocytes ($79.2 \pm 21.1\%$; N.S. vs AoB). Figure 5C shows that failure to achieve significance was due to a wide scatter in istaroxime effect among cells. Rather than being casually variable, istaroxime effect was inversely related to the Ca_{SRT} level measured in control condition, to steeply increase for values below $20 \mu\text{mol/L}$ cyt. Stimulation of SR Ca^{2+} uptake by istaroxime was fully preserved in AoB myocytes, in which baseline SR function was depressed (Fig 6B). Istaroxime effect on the increase in Ca^{2+} transient amplitude during the reloading protocol was actually larger in AoB than in sham myocytes (two-way ANOVA, $p < 0.05$). For the other parameters (τ_{decay} and CICR-gain) istaroxime effect, although highly significant in both groups, was not significantly different between sham and AoB myocytes, probably due to the larger scatter of values. The absolute SR performance achieved under istaroxime in AoB myocytes approached that observed in sham myocytes (Fig 6B), to indicate substantial recovery of AoB-induced dysfunction.

CICR-gain (measured by protocol 1) was similarly increased by istaroxime in AoB and sham myocytes (Fig 7). The slope of I_{NCX}/Ca_f relationship ($+173 \pm 89\%$) and Ca_{rest} ($+29 \pm 5\%$) were also increased

by istaroxime, the effect was again similar between sham and AoB myocytes (Fig 8).

Discussion

Features of the AoB model

The pressure overload model used in the present study has been previously characterized in vivo at 12 weeks after banding of the ascending aorta, with findings compatible with left ventricular hypertrophy and mild failure¹⁶; the present ex vivo observations (table 2) are substantially in agreement with in vivo ones. The HW/BW ratio and C_m were consistently increased after AoB, thus reflecting clear-cut myocardial hypertrophy in all cases. Lung congestion was present in a minority of cases. The absence of mortality in the AoB groups rules out the possibility that the hearts used for cell studied may come from a surviving subpopulation, i.e. one with particularly mild abnormalities. Cardiac decompensation observed in the present work is mild as compared to that observed in guinea-pigs studied up to 8 weeks after banding of descending aorta^{17;18}.

The main functional derangement observed in myocytes from AoB animals concerned SR Ca^{2+} uptake function. This was manifested by a marked depression of SR reloading (after caffeine-induced depletion) (Fig 2). Conversely, reduction in SR Ca^{2+} content was relatively milder (-32%; Fig 1) and CICR-gain during steady-state stimulation under normal Tyrode superfusion was unchanged (Fig 3). Considering that SR reloading was measured starting from very a low cell Ca^{2+} content and during NCX blockade, the discrepancy might suggest that

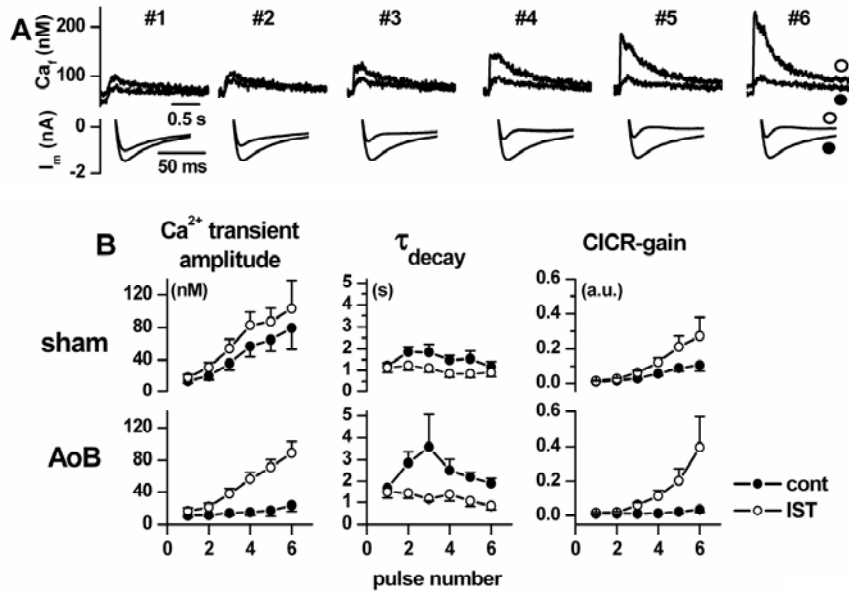


Figure 6: Istaroxime effects in sham vs AoB groups: SR function with blocked NCX. A) Example of free cytosolic Ca²⁺ concentration (Ca_i) and membrane current (I_m) recorded in a AoB myocyte during SR reloading after caffeine-induced SR depletion in control (cont, ●) and after istaroxime superfusion (IST 4 μM, ○); recordings were performed in the absence of NCX function (Na⁺ free Tyrode and pipette solutions); the protocol is outlined in figure 2. B) Average values of Ca²⁺ transient parameters measured during each of the first 6 pulses (#1 to #6) of the stimulation train in cont (●) and after IST superfusion (○), in sham (N = 11) and AoB (N = 8) myocytes. The decay time constant (τ_{decay}) was estimated by a monoexponential fit of the Ca²⁺ transient decay; CICR-gain (measured as the ratio between the Ca²⁺ transient amplitude and the peak inward current) was expressed in arbitrary units (a.u). Significance of istaroxime effects was tested by two-way ANOVA on all variables for both sham and AoB groups (see text).

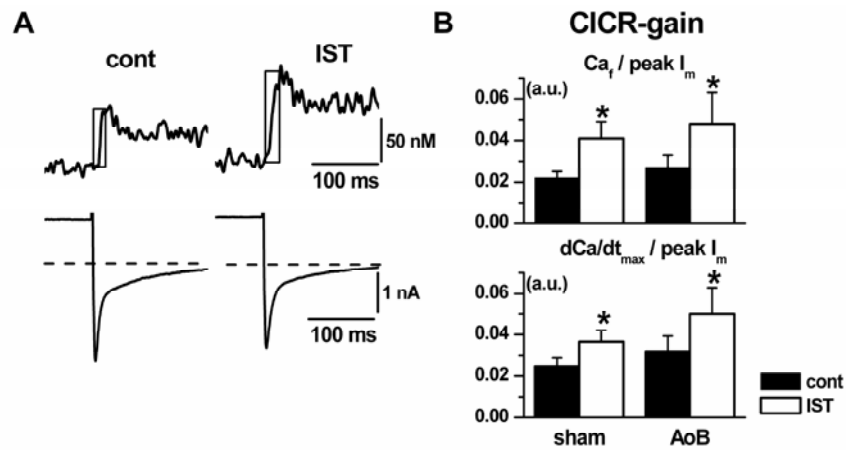


Figure 7: Istaroxime effects in sham vs AoB groups: CICR-gain. A) Free cytosolic Ca^{2+} concentration (Ca_i) and membrane current (I_m) simultaneously recorded during voltage steps (from -40 to 0 mV for 200 ms) in a sham myocyte, in control (cont) and after istaroxime superfusion (IST 4 μ M). B). Average values of CICR-gain (calculated according to two methods and expressed in arbitrary units, a.u., see Methods) in control and after IST superfusion in sham (N = 13) and AoB (N = 17) myocytes; dCa/dt_{max} was calculated during the rising phase of the Ca^{2+} transient (boxes in panel A). * = $p < 0.05$ vs cont.

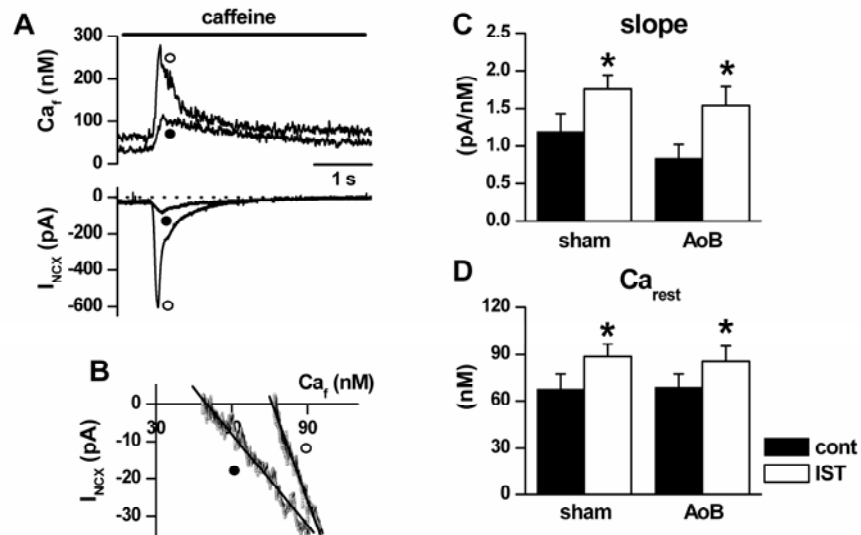


Figure 8: Istaroxime effects in sham vs AoB groups: NCX function. A) Free cytosolic Ca^{2+} concentration (Ca_f) and the $\text{Na}^+/\text{Ca}^{2+}$ exchanger current (I_{NCX}) simultaneously recorded in a sham myocyte during caffeine superfusion (holding potential -80 mV) in control (cont, ●) and after istaroxime superfusion (IST $4 \mu\text{M}$, ○); Ca_f and I_{NCX} traces recorded in cont and IST were time aligned for clarity; I_{NCX} traces were also offset to 0 level at the end of caffeine pulse. B) $I_{\text{NCX}}/\text{Ca}_f$ relationships and the linear interpolation of the points in the final third of Ca^{2+} transient relaxation (continuous lines). C), D) Average results of the slope of the $I_{\text{NCX}}/\text{Ca}_f$ relationship and resting Ca^{2+} measured at -80 mV (Ca_{rest}) in cont and after IST superfusion in sham ($N = 8$) and AoB ($N = 11$) myocytes; * = $p < 0.05$ vs cont.

the derangement in SR uptake function may be unveiled by low Ca^{2+} content and partially compensated by NCX function. The observation that the reduction of SR Ca^{2+} content was not associated with a decrease in CICR-gain might suggest that the ryanodine receptor (RyR) sensitivity to cytosolic Ca^{2+} was increased in AoB myocytes, as commonly observed in the failing heart¹⁹.

Abnormality of the SR uptake function, as those detected in this study, can be due to reduced SERCA2 activity, or to increased Ca^{2+} leak through RyR channels. Previous biochemical evaluations showed that maximal ATP-ase activity of SERCA2 is indeed decreased in this model, in spite of normal expression of SERCA2 protein¹⁶. Reduced SERCA2 activity might result from an increase in the unphosphorylated (monomeric) form of PLB (with no change in the phosphorylated or pentameric fraction), previously described in this model¹⁶. In this case SERCA2 abnormality would be “functional”, rather than structural, a view also supported by the effect of istaroxime discussed below. This pattern differs from that more often described in hypertrophy, in which a decreased in SERCA2 expression contributes to downregulation of SR Ca^{2+} transport⁷.

Ca^{2+} -dependency of I_{NCX} was preserved after AoB (fig 4). This finding is apparently at variance with upregulation of NCX protein expression and enhancement of I_{NCX} reported in human heart failure^{20,21} and in hypertrophy models in various species, including guinea-pig¹⁷. While NCX protein expression was not evaluated in the present work, the functional observations are not necessarily in

contrast with previous ones in the same species. In the work on guinea-pig by Ahmmed et al.¹⁷ I_{NCX} was measured upon repolarization after long depolarizing steps (tail current). An increase in I_{NCX} tail current can be due to either genuine upregulation of NCX function, or simply to an increase in cytosolic Ca^{2+} levels achieved during the depolarizing step²². Under the conditions of the study by Ahmmed et al (CICR suppression), the latter may be justified in hypertrophied myocytes by depressed SR Ca^{2+} uptake. In the present experiments, NCX function was defined through the relationship between I_{NCX} and cytosolic Ca^{2+} , thus correcting for differences in cytosolic Ca^{2+} level. Nevertheless, in species other than guinea-pigs the same analysis detected an increase of NCX function in hypertrophy²³; thus, it is difficult to rule out that differences in NCX function between this and previous studies may be real and possibly related to the severity of hemodynamic overload.

Istaroxime effects in sham and AoB myocytes

In myocytes from sham operated animals istaroxime improved Ca^{2+} handling, as previously reported in normal hearts of the same species¹. Under ionic conditions in which all Ca^{2+} handling mechanisms were operative (normal Tyrode), istaroxime increased total SR Ca^{2+} content (Fig 5), which implies a shift of the balance between Ca^{2+} uptake by SR and Ca^{2+} extrusion from the cell. In turn, SR Ca^{2+} uptake rate reflects the balance between active Ca^{2+} transport (by SERCA2) and passive Ca^{2+} leak through RyR channels, both fluxes being enhanced by high cytosolic Ca^{2+} (ref. ^{24;25}). As shown by previous studies in intact myocytes and isolated SR vesicles, istaroxime actions include

inhibition of the Na^+/K^+ pump and stimulation of SERCA2 ATP-ase activity^{1,3} (see also the Supplemental Material). While both these actions may concur to increase SR Ca^{2+} content, the former depends on the change in NCX electrochemical equilibrium, secondary to elevation of cytosolic Na^+ . When tested under conditions of complete inhibition of NCX function (Na^+ -free conditions), istaroxime was still able to stimulate SR Ca^{2+} uptake, as reflected by an increase in the rate at which SR reloads after depletion and by an acceleration of Ca^{2+} decay after voltage-induced transients (Fig 6). These observations suggest that istaroxime-induced increase in SR Ca^{2+} content may also occur through SERCA2 stimulation, i.e. independently of Na^+/K^+ pump inhibition. Istaroxime also increased the efficacy by which Ca^{2+} influx triggers SR Ca^{2+} release (CICR-gain) (Fig 7), probably an effect secondary to the increase in luminal SR Ca^{2+} (ref. ^{3,26}). Istaroxime increased both the x-axis intercept (Ca_f at $I_{\text{NCX}}=0$) and the slope of the $I_{\text{NCX}}/\text{Ca}_f$ relationship (Fig 8). The intercept change may result from an increase in cytosolic Na^+ and was expected from istaroxime effect on the Na^+/K^+ pump³. According to previous evidence, istaroxime does not directly stimulate NCX³; thus, the increase in the slope of the $I_{\text{NCX}}/\text{Ca}_f$ relationship is more likely due to allosteric modulation of the exchanger by elevated Ca_f (ref. ²⁷). The net effect of these two changes is a reduction in the rate of Ca^{2+} extrusion through NCX at resting membrane potential (-80 mV).

The rather severe SR dysfunction observed after AoB was almost completely reversed by istaroxime (Figs 5 and 6). This implies that the dysfunction was exclusively “functional” and is consistent with the lack of SERCA2 protein downregulation in this model¹⁶.

Istaroxime effect in skeletal vs cardiac SR microsomes

The ability of istaroxime to recover the SR abnormality in AoB myocytes suggests that this agent may interfere with SERCA modulation by PLB. This is also consistent with the finding that istaroxime stimulates SERCA2 in cardiac microsomes from healthy guinea pig by increasing its affinity for cytosolic Ca^{2+} (ref. ^{1;16}) (see also Supplemental Material and Supplemental Figure 4), which is limited by the interaction with PLB²⁸.

The observation, reported in the Supplemental Material that istaroxime was unable to increase SERCA activity in skeletal muscle microsomes, which are naturally devoid of PLB, provides a preliminary support to this view (Supplemental Figures 3-4). Albeit suggestive, this observation may not be conclusive and further experiments with a different strategy may be required to confirm the hypothesis.

Practical implications

The majority of evidence available to date, mostly from studies in transgenic animals, identifies recovery of SR Ca^{2+} uptake function as a promising therapeutic strategy in heart failure^{29;30}; however, adverse effects have also been reported^{31;32}. The net outcome of this approach probably depends on the extent of SR uptake enhancement, which may be difficult to adjust if gene-therapy is used. Under this aspect, availability of pharmacological tools for modulation of SR function would be highly desirable; however, it is unclear whether deranged SR function can be recovered by pharmacological means. Previous studies in animal models^{4;5;16} and man⁶ showed that the positive

inotropic effect of istaroxime is retained in the failing myocardium, but it was unknown whether stimulation of SR Ca^{2+} uptake could still contribute to it. The present results not only prove that this is indeed the case, but show that almost complete recovery of failing SR uptake function might be achieved by pharmacological means. Beside contractility, SR function may also affect myocardial electrical stability. Istaroxime is also a Na^+/K^+ pump inhibitor, but it is definitely less proarrhythmic than digoxin in animal studies^{2,3} and preliminary clinical evidence corroborates this finding^{6,33}. The electrophysiological actions of the two substances have been thoroughly compared³ and the only mechanism found to account for the different arrhythmogenicity is stimulation of SR Ca^{2+} uptake¹. This suggests that contractile recovery is not the only goal which may be achieved by modulation of SR function. The mechanism by which SR stimulation by istaroxime improves electrical stability is currently under evaluation.

Study limitations

In the specific hypertrophy model used by this study, decreased SERCA2 activity occurs in the presence of normal SERCA2 protein expression¹⁶ and this may represent a prerequisite for functional recovery by pharmacological means. This might prevent full extrapolation of the present findings to conditions in which SERCA2 expression is reduced. Nevertheless, a decrease in the ratio between SERCA2 and (unphosphorylated) PLB is general feature of the failing myocardium³⁰, thus suggesting that functional downregulation may have a general role in SR dysfunction. Thus, significant, even if

incomplete, recovery might theoretically be achieved by pharmacological means in most cases.

Acknowledgements

We thank Giuseppe Bianchi for providing constructive discussion throughout the execution of the study, Bruno Gavillet for reviewing the manuscript, Fiorentina Palazzo and Barbara Moro for guinea pig aortic banding, and Mara Ferrandi for Western blot experiments (Supplemental Fig. 3)

Supplemental material

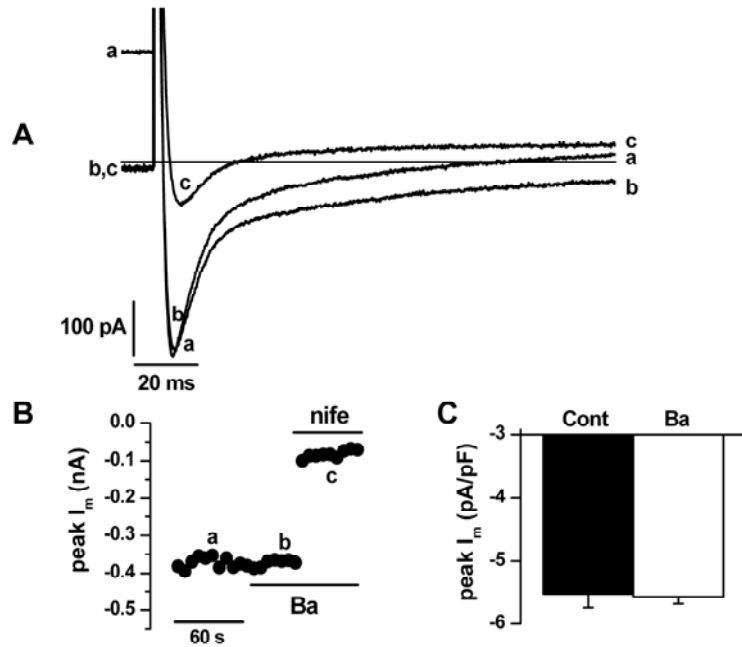
Peak inward current reflects Ca²⁺ influx:

Accurate measurement of I_{CaL} requires intracellular K^+ substitution by Cs^+ , that was not implemented in the present study because Cs^+ affects SR function¹⁰. In the present study Ca^{2+} influx was estimated from the peak inward current with the only purpose of computing CICR gain.

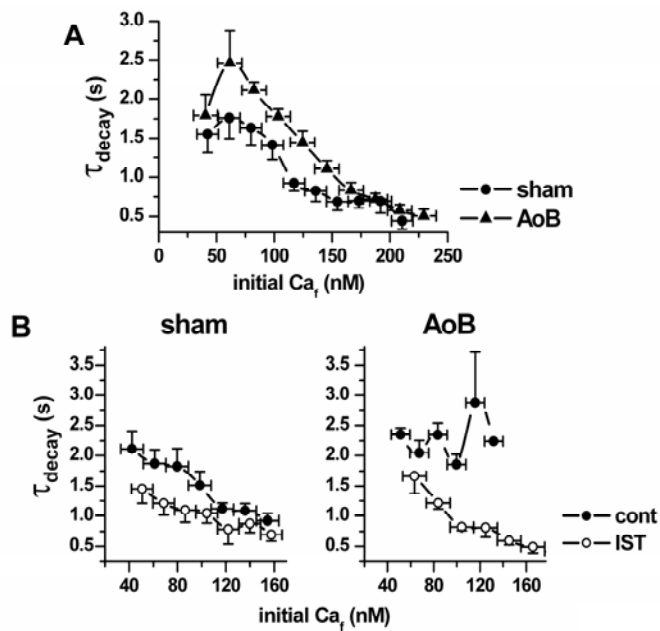
As shown in the Supplemental Figure 1, the inactivation time-course of the inward current measured at 0 mV (from a holding potential of -40 mV) was modified by aspecific K^+ channels blockade with 1 mM barium; however, the peak inward current amplitude was not significantly altered by K^+ channels blockade. Thus, only the peak value of inward current may accurately reflect Ca^{2+} influx even in the absence of K^+ channels blockade.

Analysis of Ca²⁺ decay rate as a function of initial Ca²⁺ level:

To isolate the SR function we analyzed the SR Ca^{2+} uptake rate in the absence of the Na^+/Ca^{2+} exchanger (protocol 2). In this study, we showed that the SR reloading process was markedly slowed and the τ_{decay} of the Ca^{2+} transient was uniformly increased over the whole reloading train in AoB myocytes (Fig 2); istaroxime sharply accelerated Ca^{2+} decay in AoB as in sham myocytes (Fig 6). Since SERCA function is regulated by cytosolic Ca^{2+} (ref. ¹⁴), changes in Ca^{2+} decay rate might simply reflect changes in cytosolic Ca^{2+} . Thus, dependence of Ca^{2+} decay rate on initial Ca^{2+} level was investigated.



Supplemental figure 1: Peak inward current analysis following K^+ channels blockade. **A)** representative traces recorded at 0 mV from an holding potential of -40 mV, in control (Tyrode solution, a), during aspecific K^+ channels blockade (1 mM $BaCl_2$, b) and after selective I_{CaL} blockade by 5 μ M nifedipine (c). **B)** peak inward current measurement at each voltage stimulus (cycle length = 6s) in all experimental condition. **C)** average results obtained in 3 cells.



Supplemental figure 2: Dependence of Ca^{2+} decay rate on initial Ca^{2+} level. Ca^{2+} decay time constant (τ_{decay}) measured from the experiments shown in figures 2 (panel **A**) and 6 (panel **B**) are plotted against Ca^{2+} concentration at the beginning of the decay phase (initial Ca^{2+}). Initial Ca^{2+} values were binned and the median of each bin is reported on the abscissa. **A**) AoB (▲) versus sham (●). **B**) istaroxime (open symbol) versus control in sham and AoB myocytes. Significance of AoB- and istaroxime-induced changes were detected by two-way ANOVA ($p < 0.05$).

The results show that the changes in τ_{decay} observed after AoB (Fig 2) and as a consequence of istaroxime superfusion (Fig 6) persisted after normalization for the initial Ca^{2+} level and can thus be attributed to a direct effect (Supplemental Figure 2).

Istaroxime effect on SERCA activity in SR microsomes preparations

The ability of istaroxime to stimulate SERCA2 activity by increasing its affinity for ambient Ca^{2+} was previously demonstrated in guinea-pig cardiac microsomes¹⁶. The skeletal muscle isoform of SERCA (SERCA1) has high structural and functional homology with SERCA2, but it is expressed in the absence of PLB³⁴. Thus, if the molecular target of istaroxime were PLB, the drug should not affect SERCA1 activity in SR microsomes prepared from skeletal muscle. In order to preliminarily test the hypothesis that istaroxime may stimulate SERCA2 by limiting its interaction with PLB, we tested the effects of istaroxime on the Ca^{2+} -dependency of SERCA activity of skeletal muscle SR microsomes.

Microsome preparations

To obtain SERCA1 and SERCA2 enriched microsomes, specimens of guinea-pig skeletal and left ventricular muscle were respectively excised, washed in ice-cold saline solution and homogenized in 4 volumes of 10 mM NaHCO_3 , pH 7, 1 mM PMSF, 10 $\mu\text{g}/\text{ml}$ aprotinin and leupeptin and centrifuged at 12.000g and 4°C for 15 min. Supernatants were filtered through four sheets of cheesecloth and

centrifuged at 100000g and 4°C for 30 minutes. Contractile proteins were extracted by suspending the pellets with 0.6 M KCl, 30 mM Histidine, pH 7 and further centrifugation at 100000g. Final pellets were reconstituted with 0.3 M Sucrose, 30 mM Histidine, pH 7 and stored in aliquots at -80°C (ref. ³⁵).

Ca-ATPase activity measurement

Ca-ATPase activity was measured "in vitro" as the rate of ³²P-ATP hydrolysis at different free Ca²⁺ concentrations (10-3000 nM). Two µg of the microsome preparation were pre-incubated with 100 nM or 200 nM thapsigargin for 5 minutes at 4°C in 80 µl of a solution containing 100 mM KCl, 5 mM MgCl₂, 1 µM A23187, 20 mM Tris, pH 7.5. After the pre-incubation, 20 µl of a 5 mM (final concentration) Tris-ATP solution containing 50 nCi of ³²P-ATP (0.5-3 Ci/mmol, Amersham) were added. ATP hydrolysis was followed for 15 minutes at 37°C and was stopped by acidification with 100 µl of ice-cold perchloric acid 20% v/v. ³²P was separated by centrifugation with activated charcoal (Norit A, SERVA) and the radioactivity was measured by liquid scintillation counting in beta counter (LS 5000 CE Beckman). SERCA-dependent activity was identified as the portion of total hydrolytic activity inhibited by 1 µM Cyclopiazonic Acid (CPA).

Protein quantification by Western Blotting analysis

Samples were separated by SDS-polyacrylamide gel electrophoresis (Criterion XT Biorad), blotted and incubated at 4°C with specific primary antibodies (goat anti-SERCA, Santa Cruz Biotechnology, CA, and monoclonal anti-PLB, UBI, Charlottesville, VA), followed by 1h

incubation with fluorescent secondary antibodies and analyzed by Odyssey Infrared Imaging detection system (LI-COR).

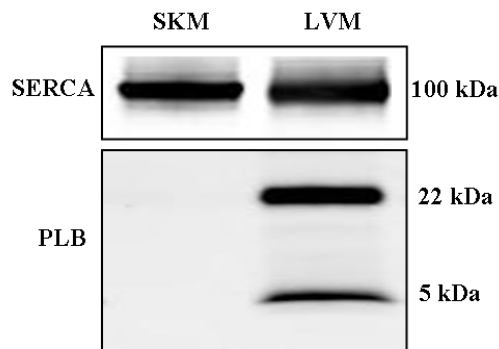
Results

Western blot analysis of PLB protein content of skeletal muscle microsomes confirmed that PLB was absent from this preparation and large abundant in cardiac muscle microsomes (Supplemental Figure 3).

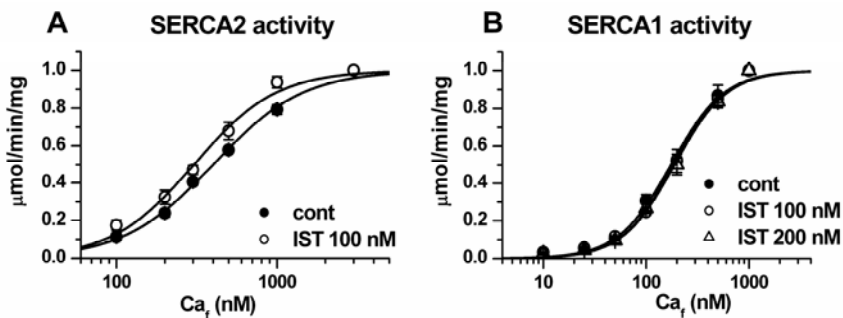
The effect of istaroxime (100 and 200 nM) on the Ca^{2+} dependency of SERCA1 ATP-ase activity in skeletal muscle microsomes is shown in Supplemental Figure 4 (right panel). Data points represent the average of 3 determinations from 2 preparations. The parameters estimated under each experimental condition by fitting the data points with the Hill equation are listed in table 1S. The curves recorded in the presence of istaroxime are almost superimposed to the one recorded in control condition. None of the Hill equation parameters was significantly affected by istaroxime at both tested concentrations.

As a comparison, istaroxime (100 nM) effect on SERCA2 activity in guinea-pig cardiac microsomes is also shown in Supplemental Figure 4 (left panel). Data points represent the average of 9 determinations from 8 preparations. Average results for this experiment are listed in table 2S. As previously reported¹⁶, istaroxime increases Ca^{2+} affinity of the SERCA2-PLB complex without affecting V_{max} and the Hill number (n).

All together, these preliminary results support the hypothesis that istaroxime increases SERCA2 activity in cardiac myocytes by



Supplemental figure 3: SERCA and PLB in SR microsomes. Western blot analysis of SERCA and PLB protein levels in guinea-pig skeletal (SKM) and left ventricular (LVM) muscle microsomes.



Supplemental figure 4: Istaroxime effect on SERCA activity in SR microsomes. Istaroxime effect on the Ca^{2+} dependency of SERCA activity in the guinea-pig cardiac (A) and skeletal (B) muscle microsomes. Average results are plotted normalized to the V_{max} values. Experimental data were best fitted using the Hill equation (continuous lines).

modulating the SERCA2–PLB interaction probably relieving the inhibitory effect of PLB. Albeit suggestive, this observation may not be conclusive and further experiments with a different strategy may be required to confirm the hypothesis.

Reference List of Chapter 2

1. Rocchetti M, Besana A, Mostacciuolo G, Micheletti R, Ferrari P, Sarkozi S, Szegedi C, Jona I, Zaza A. Modulation of sarcoplasmic reticulum function by Na⁺/K⁺ pump inhibitors with different toxicity: Digoxin and PST2744 [(E,Z)-3-((2-aminoethoxy)imino)androstane-6,17-dione hydrochloride]. *J Pharmacol Exp Ther.* 2005;313:207-215.
2. Micheletti R, Mattera GG, Rocchetti M, Schiavone A, Loi MF, Zaza A, Gagnol RJP, De Munari S, Melloni P, Carminati P, Bianchi G, Ferrari P. Pharmacological profile of the novel inotropic agent (E,Z)-3-((2-aminoethoxy)imino)androstane-6,17-dione hydrochloride (PST2744). *J Pharmacol Exp Ther.* 2002;303:592-600.
3. Rocchetti M, Besana A, Mostacciuolo G, Ferrari P, Micheletti R, Zaza A. Diverse toxicity associated with cardiac Na⁺/K⁺ pump inhibition: Evaluation of electrophysiological mechanisms. *J Pharmacol Exp Ther.* 2003;305:765-771.
4. Mattera GG, Lo Giudice P, Loi FMP, Vanoli E, Gagnol JP, Borsini F, Carminati P. Istaroxime: A new luso-inotropic agent for heart failure. *Am J Cardiol.* 2007;99:33A-40A.
5. Sabbah HN, Imai M, Cowart D, Amato A, Carminati P, Gheorghiade M. Hemodynamic properties of a new-generation positive luso-inotropic agent for the acute treatment of advanced heart failure. *Am J Cardiol.* 2007;99:41A-46A.
6. Ghali JK, Smith WB, Torre-Amione G, Haynos W, Rayburn BK, Amato A, Zhang D, Cowart D, Valentini G, Carminati P, Gheorghiade M. A phase 1-2 dose-escalating study evaluating the safety and tolerability of istaroxime and specific effects on electrocardiographic and hemodynamic parameters

in patients with chronic heart failure with reduced systolic function. *Am J Cardiol.* 2007;99:47A-56A.

7. Bers DM. Altered cardiac myocyte Ca regulation in heart failure. *Physiology (Bethesda)*. 2006;21:380-387.
8. Zaza A, Rocchetti M, Brioschi A, Cantadori A, Ferroni A. Dynamic Ca²⁺-induced inward rectification of K⁺ current during the ventricular action potential. *Circ Res.* 1998;82:947-956.
9. Zicha S, Moss I, Allen B, Varro A, Papp J, Dumaine R, Antzelevich C, Nattel S. Molecular basis of species-specific expression of repolarizing K⁺ currents in the heart. *Am J Physiol Heart Circ Physiol.* 2003;285:H1641-H1649.
10. Kawai M, Hussain M, Orchard CH. Cs⁺ inhibits spontaneous Ca²⁺ release from sarcoplasmic reticulum of skinned cardiac myocytes. *Am J Physiol.* 1998;275:H422-H430.
11. Grynkiewicz G, Poenie M, Tsien RY. A new generation of Ca²⁺ indicators with greatly improved fluorescence properties. *J Biol Chem.* 1985;260:3440-3450.
12. Sipido KR, Callewaert G. How to measure intracellular [Ca²⁺] in single cardiac cells with fura-2 or indo-1. *Cardiovasc Res.* 1995;29:717-726.
13. Bers DM. Excitation-contraction coupling and cardiac contractile force. 2002. Kluwer Academic Publishers, Boston.
14. Bers DM, Berlin JR. Kinetics of [Ca]_i Decline in Cardiac Myocytes Depend on Peak [Ca]_i. *Am J Physiol Cell Physiol.* 1995;37:C271-C277.
15. Lee KS, Marban E, Tsien RW. Inactivation of calcium channels in mammalian heart cells: joint dependence on membrane potential and intracellular calcium. *J Physiol.* 1985;364:395-411.

16. Micheletti R, Palazzo F, Barassi P, Glacalone G, Ferrandi M, Schiavone A, Moro B, Parodi O, Ferrari P, Bianchi G. Istaroxime, a stimulator of sarcoplasmic, reticulum calcium adenosine triphosphatase isoform 2a activity, as a novel therapeutic approach to heart failure. *Am J Cardiol.* 2007;99:24A-32A.
17. Ahmmed GU, Dong PH, Song GJ, Ball NA, Xu YF, Walsh RA, Chiamvimonvat N. Changes in Ca²⁺ cycling proteins underlie cardiac action potential prolongation in a pressure-overloaded guinea pig model with cardiac hypertrophy and failure. *Circ Res.* 2000;86:558-570.
18. Kiss E, Ball NA, Kranias EG, Walsh RA. Differential changes in cardiac phospholamban and sarcoplasmic reticular Ca(2+)-ATPase protein levels. Effects on Ca²⁺ transport and mechanics in compensated pressure-overload hypertrophy and congestive heart failure. *Circ Res.* 1995;77:759-764.
19. Yano M, Yamamoto T, Ikemoto N, Matsuzaki M. Abnormal ryanodine receptor function in heart failure. *Pharmacol Ther.* 2005;107:377-391.
20. Pieske B, Maier LS, Bers DM, Hasenfuss G. Ca²⁺ handling and sarcoplasmic reticulum Ca²⁺ content in isolated failing and nonfailing human myocardium. *Circ Res.* 1999;85:38-46.
21. Studer R, Reinecke H, Bilger J, Eschenhagen T, Bohm M, Hasenfuss G, Just H, Holtz J, Drexler H. Gene expression of the cardiac Na(+)-Ca²⁺ exchanger in end-stage human heart failure. *Circ Res.* 1994;75:443-453.
22. Barceñas-Ruiz L, Beuckelmann DJ, Wier WG. Sodium-calcium exchange in heart: membrane currents and changes in [Ca²⁺]_i. *Science.* 1987;238:1720-1722.
23. Diaz ME, Graham HK, Trafford AW. Enhanced sarcolemmal Ca²⁺ efflux reduces sarcoplasmic reticulum Ca²⁺ content and systolic Ca²⁺ in cardiac hypertrophy. *Cardiovasc Res.* 2004;62:538-547.

24. Meissner G, Henderson JS. Rapid Calcium Release from Cardiac Sarcoplasmic-Reticulum Vesicles Is Dependent on Ca²⁺ and Is Modulated by Mg²⁺, Adenine-Nucleotide, and Calmodulin. *J Biol Chem.* 1987;262:3065-3073.
25. Shannon TR, Ginsburg KS, Bers DM. Reverse mode of the sarcoplasmic reticulum calcium pump and load-dependent cytosolic calcium decline in voltage-clamped cardiac ventricular myocytes. *Biophys J.* 2000;78:322-333.
26. Xu L, Meissner G. Regulation of cardiac muscle Ca²⁺ release channel by sarcoplasmic reticulum luminal Ca²⁺. *Biophys J.* 1998;75:2302-2312.
27. Weber CR, Ginsburg KS, Philipson KD, Shannon TR, Bers DM. Allosteric regulation of Na/Ca exchange current by cytosolic Ca in intact cardiac myocytes. *J Gen Physiol.* 2001;117:119-131.
28. Waggoner JR, Huffman J, Froehlich JP, Mahaney JE. Phospholamban inhibits Ca-ATPase conformational changes involving the E2 intermediate. *Biochemistry.* 2007;46:1999-2009.
29. Schmidt AG, Edes I, Kranias EG. Phospholamban: a promising therapeutic target in heart failure? *Cardiovasc Drugs Ther.* 2001;15:387-396.
30. Haghighi K, Gregory KN, Kranias EG. Sarcoplasmic reticulum Ca-ATPase-phospholamban interactions and dilated cardiomyopathy. *Biochem Biophys Res Commun.* 2004;322:1214-1222.
31. Chen Y, Escoubet B, Prunier F, Amour J, Simonides WS, Vivien B, Lenoir C, Heimburger M, Choqueux C, Gellen B, Riou B, Michel JB, Franz WM, Mercadier JJ. Constitutive cardiac overexpression of sarcoplasmic/endoplasmic reticulum Ca²⁺-ATPase delays myocardial failure after myocardial infarction in rats at a cost of increased acute arrhythmias. *Circulation.* 2004;109:1898-1903.

32. Vangheluwe P, Tjwa M, Van den Bergh A, Louch WE, Beullens M, Dode L, Carmeliet P, Kranias E, Herijgers P, Sipido KR, Raeymaekers L, Wuytack F. A SERCA2 pump with an increased Ca²⁺ affinity can lead to severe cardiac hypertrophy, stress intolerance and reduced life span. *J Mol Cell Cardiol.* 2006;41:308-317.
33. Ferrari P, Micheletti R, Valentini G, Bianchi G. Targeting SERCA2a as an innovative approach to the therapy of congestive heart failure. *Med Hypotheses.* 2007;68:1120-1125.
34. Periasamy M, Kalyanasundaram A. SERCA pump isoforms: their role in calcium transport and disease. *Muscle Nerve.* 2007;35:430-442.
35. Nediani C, Fiorillo C, Marchetti E, Pacini A, Liguri G, Nassi P. Stimulation of cardiac sarcoplasmic reticulum calcium pump by acylphosphatase. Relationship to phospholamban phosphorylation. *J Biol Chem.* 1996;271:19066-19073.

